Supplementary material to "Robust 3D gravity gradient inversion by planting anomalous densities" by Leonardo Uieda and Valéria C. F. Barbosa*

Leonardo Uieda[1] and Valéria C. F. Barbosa[2]

Observatório Nacional, Rio de Janeiro, Brazil. Contact e-mail: [1] leouieda@gmail.com ; [2] valcris@on.br

May 9, 2012

ABSTRACT

We provide supplementary material to "Robust 3D gravity gradient inversion by planting anomalous densities" by Leonardo Uieda and Valéria C. F. Barbosa. The material included are: (1) plots of the predicted and synthetic g_{yy} and g_{yz} components from the section "Application to synthetic data", (2) plots of the results of the sensitivity analysis to uncertainties in the density-contrast value of the seeds, (3) the contour maps of the synthetic and predicted data for the synthetic tests in the "Sensitivity analysis" section, and (4) a synthetic test illustrating the use of the ℓ_2-norm of the residual vector in the data-misfit function.

MISSING FIGURES FROM "APPLICATION TO SYNTHETIC DATA"

Figure 1 shows the synthetic (color-scale maps) and predicted (black contour lines) data of the g_{yy} and g_{yz} components of the gravity gradient tensor. The synthetic data were produced by multiple targeted and non-targeted sources shown in Figure 5a of Uieda and Barbosa (2012). The predicted data were produced by the inversion result shown in Figure 5c of Uieda and Barbosa (2012).

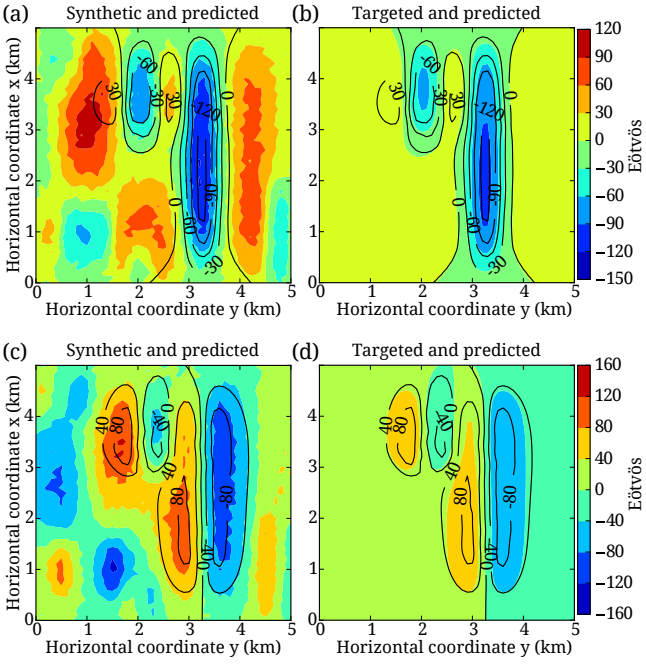

Figure 1: Test with synthetic data produced by multiple targeted and non-targeted sources shown in Figure 5a of Uieda and Barbosa (2012). (a) Synthetic noise-corrupted data (color-scale map) of the g_{yy} component of the gravity gradient tensor produced by targeted and non-targeted sources. (b) Synthetic data (color-scale map) of the g_{yy} component produced by the targeted sources only. (c) Synthetic noise-corrupted data (color-scale map) of the g_{yz} component of the gravity gradient tensor produced by targeted and non-targeted sources. (d) Synthetic data (color-scale map) of the g_{yz} component produced by the targeted sources only. In a-d the predicted data (black contour lines) are produced by the inversion result shown in Figure 5c of Uieda and Barbosa (2012).

MISSING FIGURES FROM "SENSITIVITY ANALYSIS"

Here, we provide additional figures for the section "Sensitivity analysis" of Uieda and Barbosa (2012). Figure 2 shows the results obtained by using correct seed locations but a density contrast lower than the true one. The estimated density-contrast distribution (light gray prisms in Figure 2) has a larger volume than the true source (black outlines in Figure 2).

Figure 3 shows the results obtained by using correct seed locations but a density contrast larger than the true one. The estimated density-contrast distribution (dark gray prisms in Figure 3) has a smaller volume than the true source (black outlines in Figure 3).

Figure 4 shows the synthetic (color-scale maps) and predicted (black contour lines) data of the g_{zz} component of

*Submitted to journal *GEOPHYSICS* on October 3, 2011.

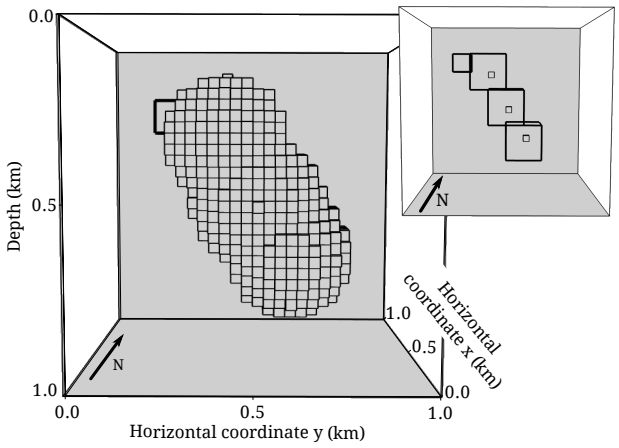

Figure 2: Analysis of the sensitivity to uncertainties in the location of the seeds. Test using ideal seed locations but a density contrast of 0.3 g/cm^3, which is smaller than the true one (1.0 g/cm^3). The outline of the true sources are shown in solid black lines. The inversion result is shown as light gray prisms. Prisms with zero density contrast are not shown. The inset shows the three seeds used in the inversion (light gray prisms) and the outline of the true sources (solid black lines). The location of the seeds was chosen in order to outline the correct dip of the large dipping source (targeted source).

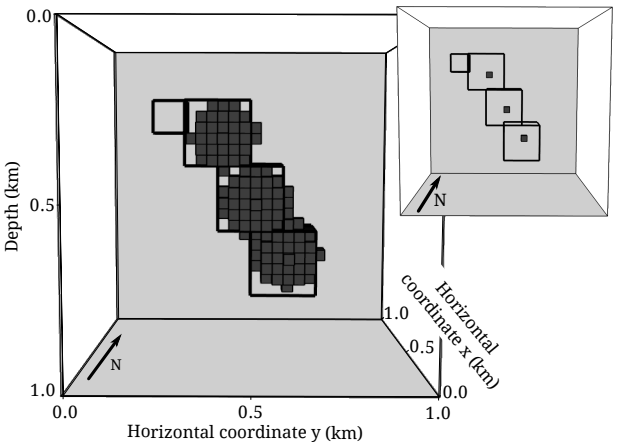

Figure 3: Analysis of the sensitivity to uncertainties in the location of the seeds. Test using ideal seed locations but a density contrast of 1.5 g/cm^3, which is larger than the true one (1.0 g/cm^3). The outline of the true sources are shown in solid black lines. The inversion result is shown as dark gray prisms. Prisms with zero density contrast are not shown. The inset shows the three seeds used in the inversion (dark gray prisms) and the outline of the true sources (solid black lines). The location of the seeds was chosen in order to outline the correct dip of the large dipping source (targeted source).

the gravity gradient tensor for all tests in the "Sensitivity analysis" section of Uieda and Barbosa (2012).

APPLICATION TO SYNTHETIC DATA USING THE ℓ_2-NORM

Figure 5 shows a set of color-scale maps of the synthetic noise-corrupted g_{xx}, g_{xy}, g_{xz}, g_{yy}, g_{yz}, and g_{zz} components of the gravity gradient tensor calculated at 150 meter height. The data were contaminated with pseudorandom Gaussian noise with zero mean and 5 Eötvös standard deviation. Each tensor component was calculated on a regular grid of 26×26 observation points in the x- and y-directions, totaling a data set of 4,056 observations, with a grid spacing of 0.2 km along both directions. The synthetic data were produced by four closely separated sources (Figure 6a). These sources are rectangular parallelepipeds with different sizes and depths and with density contrasts ranging from -1 g/cm^3 to 1 g/cm^3. In this test, all four sources are considered targets of the interpretation.

Because we did not consider the presence of geologic noise (non-targeted sources), the inversion was performed using the normalized ℓ_2-norm of the residual vector, instead of the ℓ_1-norm, in the data misfit function, i.e.,

$$\phi_{\alpha\beta}(\mathbf{p}) = \frac{\left|\left|\mathbf{r}^{\alpha\beta}\right|\right|_2}{\left|\left|\mathbf{g}^{\alpha\beta}\right|\right|_2} = \sqrt{\frac{\sum_{i=1}^{L}\left(g_i^{\alpha\beta} - d_i^{\alpha\beta}\right)^2}{\sum_{i=1}^{L}\left(g_i^{\alpha\beta}\right)^2}}. \qquad (1)$$

We assigned a total of 18 seeds (Figure 6b) distributed between the four sources as follows: seven for the source with density contrast of 1 g/cm^3 (in red); five for source with density contrast of -1 g/cm^3 (in blue); four for the source with density contrast of 0.7 g/cm^3 (in yellow); two for the source with density contrast of 0.9 g/cm^3 (in orange). We used an interpretative model consisting of 25,000 juxtaposed right rectangular prisms. The inversion control variables were $\mu = 0.1$ and $\delta = 0.0001$. The inversion result in Figure 6c shows that our method estimates a density-contrast distribution composed of four compact sources (i.e., without hollows) whose shapes very closely resemble the shape of the four true sources (Figure 6a), regardless of their depth, size, or density contrast. This estimated density-contrast distribution produces predicted data that fit the observed data as shown in Figure 5.

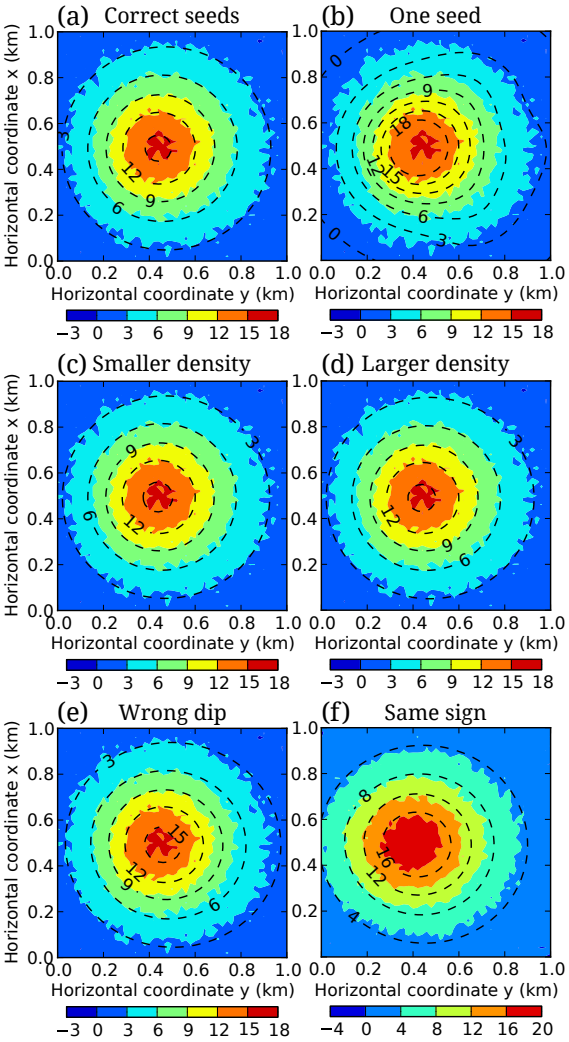

Figure 4: Sensitivity analysis of the method of planting anomalous densities. The synthetic (color-scale maps) and predicted (black contour lines) data of the g_{zz} component for all tests. (a) The test with correct seed locations and density contrasts (see Figure 6 of Uieda and Barbosa, 2012). (b) The test with only a single seed located at the top of the large dipping source (targeted source) (see Figure 8 of Uieda and Barbosa, 2012). (c) The test with correct seed locations but a density contrast lower than the true one (Figure 2). (d) The test with correct seed locations but a density contrast larger than the true one (Figure 3). (e) The test with seeds that follow an incorrect dip of the large dipping source (targeted source) (see Figure 7 of Uieda and Barbosa, 2012). (f) The test with correct seed locations and density contrasts, but with a non-targeted source with a density contrast of the same sign as that of the targeted source (see Figure 9 of Uieda and Barbosa, 2012). Color-scale units are Eötvös.

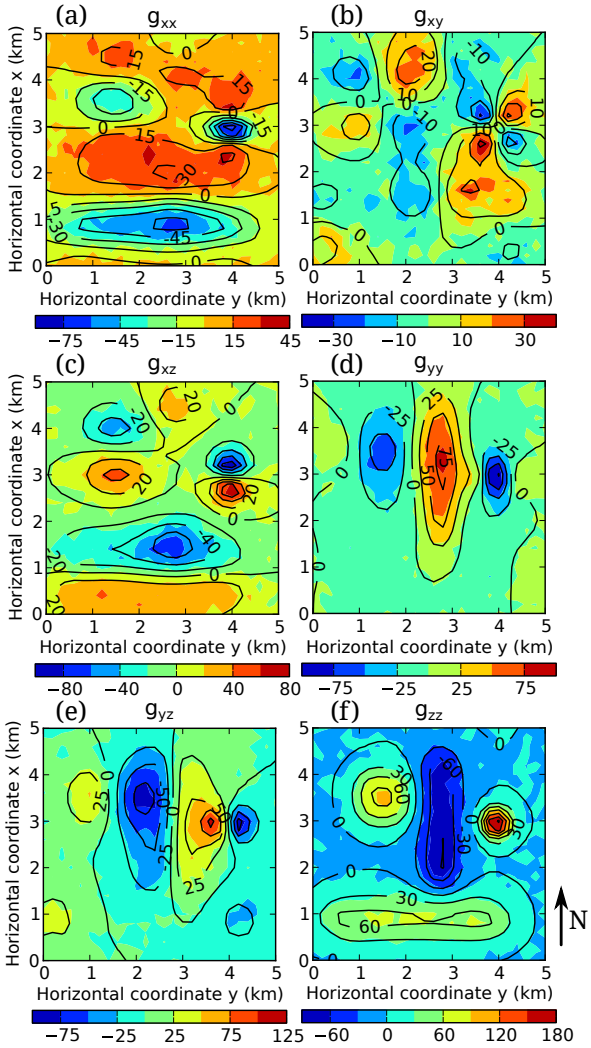

Figure 5: Test with synthetic data produced by multiple targeted sources and using the ℓ_2-norm of the residual vector. Synthetic noise-corrupted data (color-scale maps) and data predicted by the inversion result (black contour lines) of the (a) g_{xx}, (b) g_{xy}, (c) g_{xz}, (d) g_{yy}, (e) g_{yz}, and (f) g_{zz} components of the gravity gradient tensor. The synthetic data are produced by the four prisms shown in Figure 6a. The predicted is produced by the estimated density-contrast distribution shown in Figure 6c. Color-scale units are Eötvös.

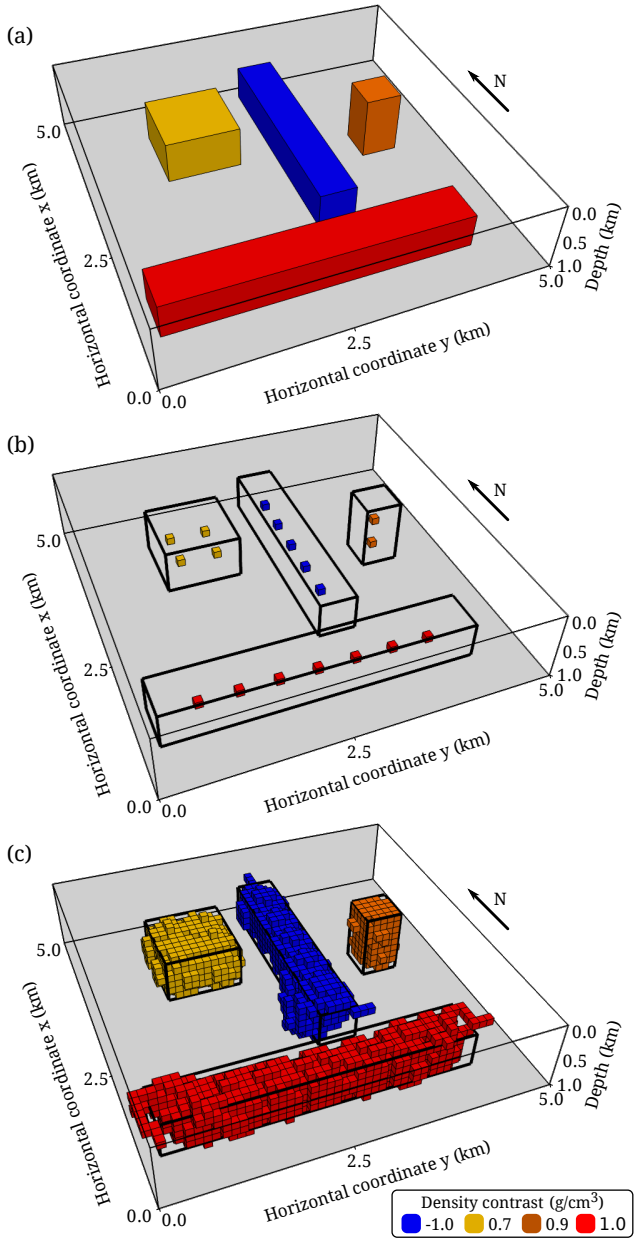

Figure 6: Test with synthetic data produced by multiple targeted sources and using the ℓ_2-norm of the residual vector. (a) Perspective view of the four targeted sources used to generate the synthetic data shown in Figure 5. (b) The 18 seeds used in the inversion. (c) Inversion result using the ℓ_2-norm of the residual vector. Prisms of the interpretative model with zero density contrast are not shown. Black lines represent the frame of the true targeted sources.